Embryogenesis and Laboratory Maintenance of the Foam-Nesting Túngara Frogs, Genus *Engystomops* (= *Physalaemus*)

Andrés Romero-Carvajal,[1] **Natalia Sáenz-Ponce,**[1] **Michael Venegas-Ferrín,**[1] **Diego Almeida-Reinoso,**[2] **Chanjae Lee,**[3] **Jennifer Bond,**[4] **Michael J. Ryan,**[4] **John B. Wallingford,**[3] **and Eugenia M. del Pino**[1]*

The vast majority of embryological research on amphibians focuses on just a single genus of frogs, *Xenopus*. To attain a more comprehensive understanding of amphibian development, experimentation on non-model frogs will be essential. Here, we report on the early development, rearing, and embryological analysis of túngara frogs (genus *Engystomops*, also called *Physalaemus*). The frogs *Engystomops pustulosus*, *Engystomops coloradorum*, and *Engystomops randi* construct floating foam-nests with small eggs. We define a table of 23 stages for the developmental period in the foam-nest. Embryos were immunostained against Lim1, neural, and somite-specific proteins and the expression pattern of RetinoBlastoma Binding Protein 6 (*RBBP6*) was analyzed by in situ hybridization. Due to their brief life-cycle, frogs belonging to the genus *Engystomops* are attractive for comparative and genetic studies of development. *Developmental Dynamics 238:1444–1454, 2009.* © 2009 Wiley-Liss, Inc.

INTRODUCTION

Many frogs deposit their eggs in the water; other frogs, however, have evolved adaptations that diminish or eliminate the aquatic requirement for reproduction (Duellman and Trueb, 1986). A deviation of the aquatic reproductive mode occurs in the túngara frogs, genus *Engystomops* (= *Physalaemus*), Leiuperidae, and consists of the formation of foam-nests that float over temporal pools. In *Engystomops pustulosus,* reproduction occurs during the rainy season; the male attracts the female with a characteristic call, and amplexus takes place. During amplexus, the male beats the egg-jelly with its legs and feet. This action produces a floating mass of white foam, in which numerous eggs are embedded (Davidson and Hough, 1969; Ryan and Rand, 2003). In this way, *E. pustulosus* eggs are placed over, and develop above, water. The strategy of placing foam-nests over temporal pools protects embryos from predators, including tadpoles of other frogs (Ryan, 1985). Moreover, the hardened surface of the nest may reflect solar radiation, decreasing heat absorption, and preventing internal desiccation. At hatching, the tadpoles fall into the water (Davidson and Hough, 1969; Ryan, 1985). *Engystomops pustulosus* is active at night and displays a complex reproductive behavior. The ecology, sexual selection, and communication strategies of this frog have been extensively studied (reviewed in Ryan,

1985; Ryan and Rand, 2003; Ron et al., 2006).

Frogs of the genus *Engystomops* inhabit the forest floor in lowland regions from Central Mexico to the Amazon basin, and the lowlands of W Ecuador and NW Peru (reviewed by Ron et al., 2006). The widely studied, *Engystomops pustulosus*, occurs at the Smithsonian Tropical Research Institute in Panamá, among other locations (Davidson and Hough, 1969; Ryan, 1985; Ron et al., 2006). Other congenerics that have been analyzed are *Engystomops coloradorum,* and *E. randi*, which inhabit the western lowlands of Ecuador (Ron et al., 2006). Mitochondrial DNA analysis of these three species revealed a close relationship. Accordingly, these frogs have been placed in the *Engystomops pustulosus* species group (Ron et al., 2006). In this study, we describe the early development of these *Engystomops* species, methods for the handling of eggs and embryos, and frog laboratory maintenance.

In the search for an anuran amphibian with synchronous oogenesis, Davidson and Hough (1969) determined that *E. pustulosus* was appropriate for developmental work. The environmental changes of wet and dry seasons were reproduced in the laboratory to analyze the modifications of oogenesis. Oogenesis changes from synchronous during the dry season to asynchronous in the wet season. During the dry season, many oocytes reach their full growth (stage 6) and remain in the ovary until reproduction is triggered by the first rains. Besides these large oocytes, only previtellogenic oocytes were detected in the ovary by the end of the dry season. In contrast, during the wet season, the full range of oocyte sizes occurs in the ovary. After the first mating of the rainy season, ovarian oocytes grow, producing oocytes of all sizes. Thereafter, in preparation for the impending mating, the largest oocytes complete their growth. This adaptation facilitates repeated mating during the wet season. Maternal transcripts are retained in *E. pustulosus* embryos to the tadpole stage (Davidson and Hough, 1969; Hough et al., 1973).

Eggs of *E. coloradorum* and *E. randi* are small and white, and resemble *Xenopus laevis* albino embryos (del Pino et al., 2007). Furthermore, as in *X. laevis,* embryonic development occurs rapidly in comparison with the slow-developing embryos of the dendrobatid frog *Colostethus* (= *Epipedobates*) *machalilla* (Grant et al., 2006), and of the marsupial frog *Gastrotheca riobambae* (del Pino et al., 2007). Tail bud stage embryos of *E. coloradorum* and *E. randi* differ from *X. laevis* embryos in their general shape, in the mode of somitogenesis, and size of cranial neural crest cell streams (del Pino et al., 2007).

Analysis of *Lim1* (*Lhx1*) gene expression at the protein level in gastrulae of *E. coloradorum* and *E. randi* allowed detection of the organizer, and of the dorsal mesoderm (del Pino et al., 2007; Venegas et al., 2009). In embryos of these frogs, elongation of the notochord overlaps with involution at the blastopore lip, as in *X. laevis* embryos (del Pino et al., 2007). In addition, in the mid gastrula, the prechordal plate and notochord were simultaneously recognized by the expression of the protein Lim1, a pattern equivalent with that of *Xlim1* mRNA expression in *X. laevis* embryos (Taira et al., 1992; 1994a,b; Venegas et al., 2009). In contrast, in embryos of the dendrobatid frog *C. machalilla,* only the prechordal plate was recognized during gastrulation. Elongation of the notochord occurred after blastopore closure in this frog (Venegas et al., 2009). This uncoupling of developmental events associates with the modular nature of frog gastrulation (Ewald et al., 2004; Moya et al., 2007; del Pino et al., 2007; Venegas et al., 2009).

In this study, we immunostained *Engystomops* embryos with several antibodies, to detect the neural tube, cranial neural crest cells, somites, pronephros, and performed in situ hybridization to analyze the expression of the RetinoBlastoma Binding Protein 6 (*RBBP6*) during development. A particular advantage for developmental studies is the brief life-cycle of these frogs, which can be as short as 4 months in *E. pustulosus* (Davidson and Hough, 1969). Our aim is to provide a methodological base-line for further comparative studies of *Engystomops* development.

RESULTS AND DISCUSSION

Engystomops Developmental Stages

Development of *E. pustulosus, E. coloradorum,* and *E. randi* embryos in the foam-nest was divided into 23 stages (st). Development in the foam-nest lasted 3 days in all of these frogs. At hatching, the foam-nest became somewhat liquid and the tadpoles moved into the water. The criteria used to define the developmental stages are given in Table 1. Developmental stages from fertilization to the early neurula were defined according to the *X. laevis* table of development (st 1–14; Nieuwkoop and Faber, 1994). Thereafter, the generalized table of frog development (Gosner, 1960) was used to stage embryos, as the embryonic morphology of *Engystomops* deviated from that of *X. laevis* embryos (Table 1) The external views of embryos are provided to complement the description of developmental stages (Figs. 1A–P, 2A–G). The free-living tadpoles were not studied.

The foam-nests of *E. pustulosus, E. coloradorum,* and *E. randi* measured about 5 cm in diameter and were 4–5 cm high. The white eggs and embryos of these frogs were effectively camouflaged in the white foam of the nest. Each nest contained 130 ± 60 eggs of 1.3-mm diameter in *E. coloradorum* (21 foam-nests with a total of 2,072 eggs)*;* and 110 ± 69 eggs of 1.1-mm diameter in *E. randi* (17 foam-nests with a total of 1,952 eggs). The foam-nests of *E. pustulosus* contain an average of 238 ± 97 eggs, based on 68 foam-nests collected in the field at the Barro Colorado Island, Panamá (Ryan, 1985). The means and standard deviations are given.

Cleavage and the Blastula (st 1–9)

External views of cleavage stage embryos are shown in Figure 1A–E, and of the blastula in Figure 1F,G. In the three species analyzed, eggs had a uniform white appearance. Therefore, the animal hemisphere could not be detected at the one-cell stage (Fig. 1A). Similarly, a gray crescent could not be detected in these pale-colored embryos. Cleavage was holoblastic

	Stage[a]		Characteristics of embryos	Age in:[b]	
E	X	G		Hours	Days
1	1	1	Fertilization (Fig. 1A).	0.0	
2	2	3	Two-cell stage.	0,3	
3	3	4	Four-cell stage (Fig. 1B).	0,6	
4	4	5	Eight-cell stage (Fig. 1C).	1	
5	5	6	Sixteen-cell stage (Fig. 1D, 3A).	1,3	
6	6	7	Thirty-two-cell stage (Fig. 1E).	1,7	
7	7	8	Large-cell blastula (Fig. 1F,3B).	3	
8	8	-	Medium-cell blastula (Fig. 1G,3C–D).	5	
9	9	9	Advanced blastula.	7.2	
10	10	10	Early gastrula. Embryos develop the dorsal blastopore lip (Figs. 1H, 3E–G).	11,5	
11	11	11	Mid gastrula with a large yolk plug that measures about one-half of the embryo's diameter (Fig. 1I).	16,2	
12	12	12	Late gastrula. The yolk plug measures one-third of the embryo's diameter or less (Figs. 1J–K, 3J–K, M).	19,7	
13	13	13	Slit blastopore stage. Some embryos have a small blastopore (Figs. 1L, 3L). The neural plate becomes visible in the late stage 13 (Fig. 3N).		1
14	14	14	Early neural fold stage (Figs. 1M, 3O, 4A)		1.1
15	15	15	Mid neural fold stage (Figs. 1N–O, 4B–H).		1.2
16		16	Closure of the neural tube (Figs. 1P, 4I–L).		1.3
17		17	Tail bud stage. The tail bud and the head region protrude beyond the yolky endoderm (Figs. 2A, 5A–F).		1.5
18		18	Muscular activity. The branchial arches protrude on the sides of the head. The cement gland is visible. The tail becomes elongated (Figs. 2B–C, 5G–H).		2
19		19	The heart beats, and the gill buds develop (not shown).		2.3
20		20	Circulation to the external gills. The first gill pair has 3 branches at this stage. Buds of the second gill pair are visible (Fig. 2D).		2.5
21		21	The first gill pair has 4 branches, and the second gill pair has 3 branches (not shown).		2.8
22		22	Blood circulation in the tail fin is detected. Five branches occur in the first pair of external gills, and 4 branches in the second pair. Embryos have a tadpole appearance (Fig. 2E).		3.1
23		23	The external gills have reached their full size. There are 6 gill branches in the first pair and 5 branches in the second pair of external gills. The opercular fold is forming. Embryos have a white appearance, although they contain some dark pigment (Fig. 2F–G).		3.4

TABLE 1. Stages of *Engystomops* Development

[a]The stages of development for *Engystomops* (E) are compared to the table of stages of *X. laevis* (X) (Nieuwkoop and Faber, 1994), and to the general staging table for frogs (G) (Gosner, 1960).
[b]Developmental times for *E. coloradorum* embryos maintained at room temperature (18–23°C) in a humid chamber.

and synchronous, and new cleavage furrows were detected every 20 min during the early cleavage cycles (Table 1). The first cleavage furrow divided the egg into two blastomeres (st. 2, not shown). At the next three cleavage cycles, new cleavage furrows developed, and divided the embryo into 4, 8 (st 3–4, Fig. 1B,C), 16, and 32 blastomeres (st 5–6; Fig. 1D,E). The planes of these cleavage furrows were equivalent with those of *X. laevis* embryos (Nieuwkoop and Faber, 1994). Animal blastomeres were smaller than the vegetal blastomeres, as shown for blastula stage embryos (st 7–9; Fig. 1F,G). Although the external appearance of

these embryos is white, dark pigment was detected around nuclei of surface cells (Fig. 1F).

Development of the blastocoel is shown in Figure 3A–C. The blastocoel was detected as a small cavity in the animal region of 8-cell-stage embryos (st 4, not shown). The blastocoel enlarged from cleavage to the onset of gastrulation (st 5–10.5; Fig. 3A–C,F). Dark pigment was detected around internal nuclei, as observed in the blastocoel roof (Fig. 3B), in the vegetal region (not shown), and in surface cells of the equatorial region (st 7; Fig. 1F). In spite of this light pigmentation, embryos had a white appearance. Transcripts of the gene *RBBP6*

were detected in animal cells of blastula stage embryos (Fig. 3D).

Gastrulation (st 10–13)

External views of the gastrula are given in Figures 1H–L, 3J. The morphology of the gastrula and the expression of the protein Lim1 are shown in Figure 3E–G, J–N. A prominent dorsal blastopore lip developed in the subequatorial region at the onset of gastrulation (st 10.5; Figs. 1H, 3E), as in embryos of *X. laevis*. Time-lapse movies of gastrulation revealed that the blastopore closes asymmetrically, moving ventrally

Developmental Dynamics

over the yolk plug as gastrulation proceeded (see Supp. Movie, which is available online), as has been observed in *X. laevis*. The archenteron was small at 10.5 (Fig. 3F,G), and bottle cells were found at the anterior tip of the archenteron (Fig. 3G), as in *X. laevis* embryos. The thickness of the blastocoel roof decreased from 5–6 cell-layers in a large-cell blastula (st 7; Fig. 3B) to 3 layers in the mid gastrula (st 11; Fig. 3H), and finally to 2 cell layers in the late gastrula (st 12; Fig. 3I). During gastrulation, the blastopore decreased in size until it was just a slit at st 13 (Fig. 1I–L). Some embryos of st 13, however, had a small yolk plug (Figs. 1L, 3L). The dorsal blastopore lip of st-10.5 embryos of *E. coloradorum* gave a positive signal for the protein Lim1 (Fig. 3E), as previously detected in *E. randi* embryos (Venegas et al., 2009). In st-12 embryos (Fig. 3J), the archenteron elongated and became inflated (Fig. 3K), and the blastocoel was still large (Fig. 3K). In slightly more advanced embryos, the archenteron was fully elongated and inflated (st 13, Fig. 3L). Small remnants of the blastocoel were detected (Fig. 3L). Elongation of the notochord started in the mid gastrula, as detected by immunostaining against the protein Lim1 (not shown). The notochord of a st-12.5 embryo is shown in Figurer 3M. The notochord was covered by endoderm in the rostral region of st-13, and -14 embryos (Fig. 3O). In the caudal region, however, the notochord was not covered by endoderm, and was exposed in the gastrocoel roof plate (Fig. 3N). These findings are consistent with the previous observation that the mode of gastrulation in *Engystomops* resembles that in *X. laevis* (del Pino et al., 2007).

Neurulation and Somite Formation (st 15–16)

The morphology of the neurula, and the expression of neural and somite markers are shown in Figure 4. External views of the neurula are given in Figures 1M–P, 4I. The neural plate was detected in st-13–14 embryos (Fig. 3N,O). The open neural folds were detected in embryos of st 14 and were clearly visible in st-15 embryos

(Fig. 1M–O). Neural folds were far more pronounced than those in *X. laevis* (Fig. 4G,H). Similarly, the gastrocoel roof plate was larger than in *X. laevis* (Figs. 3N, 4H). Transcripts of the gene *RBBP6* were restricted to the presumptive eye region (st 14, Fig. 4A). Somites were detected in st-15 embryos (Fig. 4B,C). The neural folds were positive for antigen 2G9 in st-15 embryos (Fig. 4D). The protein Lim1 was used as marker of the notochord, specific cells of the cns, and pronephros (st 15; Fig. 4E,F). The notochord was covered by endoderm in the rostral region (Fig. 4G), and it was exposed in the caudal region of st-15 embryos (Fig. 4H), as detected previously in st 13–14 (Fig. 3N,O). The neural folds gradually closed in the midline during st 16 (Figs. 1P, 4I). The streams of cranial neural crest cells were detected by the expression of antigen 2G9 in st-16 embryos (Fig. 4J). Somites were detected by immunostaining against sarcomeric meromyosin in st-15 embryos (not shown) and became more clearly detectable in st-16 embryos (Fig. 4K). Somites contain numerous cells of round shape (Fig. 4L), a feature that greatly differs from the *X. laevis* mode of somitogenesis, which involves fewer cells and cell rotation (Radice et al., 1989).

The Tail Bud and More Advanced Embryos (st 17–23)

External views of tail bud and more advanced embryos are given in Figure 2A–G. Expression of neural and somite markers are shown in Figure 5. Embryos were curved around a large yolky endoderm, and differed in shape from the elongated *X. laevis* tailbud (st 17–18; Figs. 2A–C, 5A). Prominent branchial arches were visible in living and fixed embryos (st 17; Fig. 2A–C). Transcripts of the gene *RBBP6* were detected in the neural region (Fig. 5A). After immunostaining against antigen, 2G9 rhombomeres and streams of cranial neural crest cells were visible (st. 17; Fig. 5B,C). Rhombomeres 3 and 5 were negative for antigen 2G9 (Fig. 5B,C). The branchial anterior stream was weakly stained in comparison with the mandibular, hyoid, and branchial posterior streams of cranial neural crest cells (st 17; Fig. 5C). The expression pattern of antigen 2G9 in rhombomeres

and streams of cranial neural crest cells is comparable with the previously detected expression in *G. riobambae* embryos (del Pino and Medina, 1998). The closed neural tube and optic vesicles were detected by immunostaining against NCAM (st 17; Fig. 5D). Embryos of st 17 had about 12 somites pairs, as detected by immunostaining against sarcomeric meromyosin (st 17; Fig. 5E). Pronephros, immunostained against Lim1, were larger than in st-15 embryos (Fig. 5F).

Embryos of st 18 were characterized by muscular activity (Table 1). Embryos of this stage acquired an elongated shape, somites were numerous, and the tail was longer (Fig. 5G). The heart was positive for sarcomeric meromyosin (Fig. 5G). Pronephros and pronephric ducts were fully developed in embryos of this stage (Fig. 5H). Specific cns cells were Lim1-positive (not shown). Embryos developed the cement gland, which was clearly detectable at st 18 (not shown).

Buds of the external gills developed in st-19 embryos (not shown). Further development of the external gills occurred from st 20–23 (Fig. 2D–G). At hatching, external gills were small and contained 6 gill branches in the first pair and 5 branches in the second pair (St 23; Fig. 2G). The tail became gradually elongated from st 18–23, and embryos acquired the shape of a tadpole (Fig. 2C,D,F). The opercular fold was detected in st-22–23 embryos (not shown). A remarkable feature of *Engystomops* development is the almost complete absence of dark pigment during development in the foam nest. The body and the head developed some dark pigment in st-20–23 embryos (Fig. 2D–G). In spite of the limited pigmentation, hatching embryos had a white appearance (Fig. 2F). Embryos of the three species of *Engystomops* hatched at st 23 (Table 1).

Comparison of *Engystomops* Development With Other Frogs

Early development in *E. pustulosus, E. coloradorum*, and *E. randi* greatly resembles *X. laevis* development. Eggs and early embryos are white, develop rapidly, and resemble *X. laevis* albino embryos in size and appearance. It should be noted, however, that blastomeres contain dark pig-
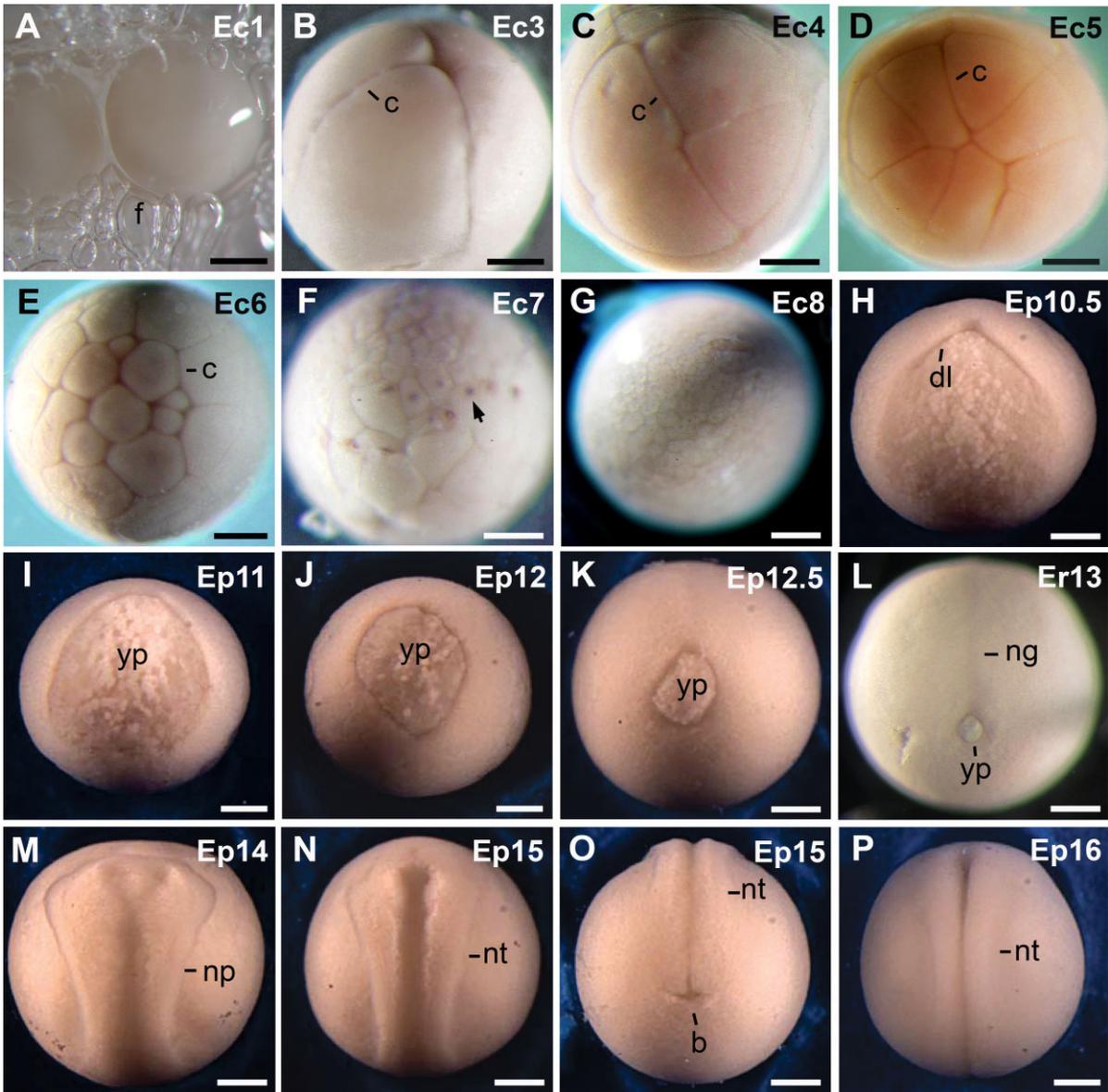
Fig. 1.

ment in the *Engystomops* species analyzed. Pigment surrounds the nuclei, instead of being localized to the surface of animal blastomeres (Figs. 1F, 3B). The patterns of cleavage, blastula formation, and gastrulation resemble closely the developmental patterns observed in *X. laevis* embryos. Elongation of the notochord overlaps with other processes of gastrulation in these rapidly developing frogs, as in *X. laevis*. In contrast, in the slow developing embryos of the dendrobatid frogs, *C. machalilla* and *G. riobambae,* the process of notochord elongation occurs after blastopore closure (del Pino,1996; Benítez and del Pino, 2002; Venegas et al., 2009). The limitations imposed by the aquatic reproductive mode of *X. laevis* and *Engystomops*
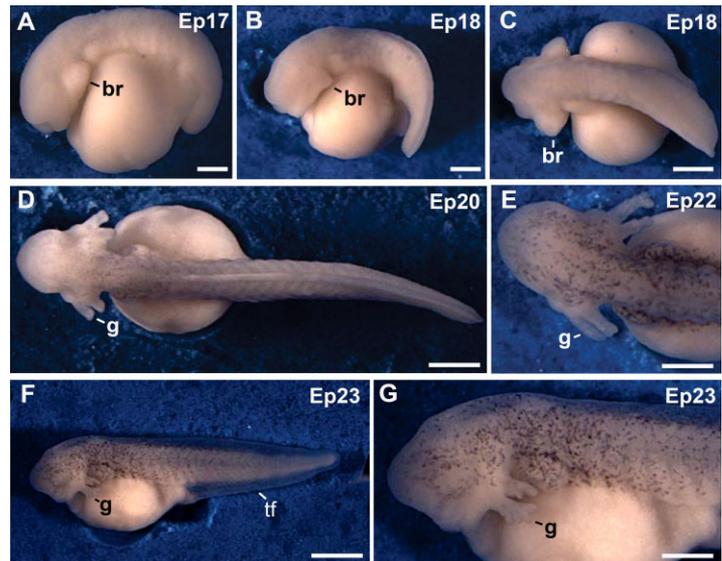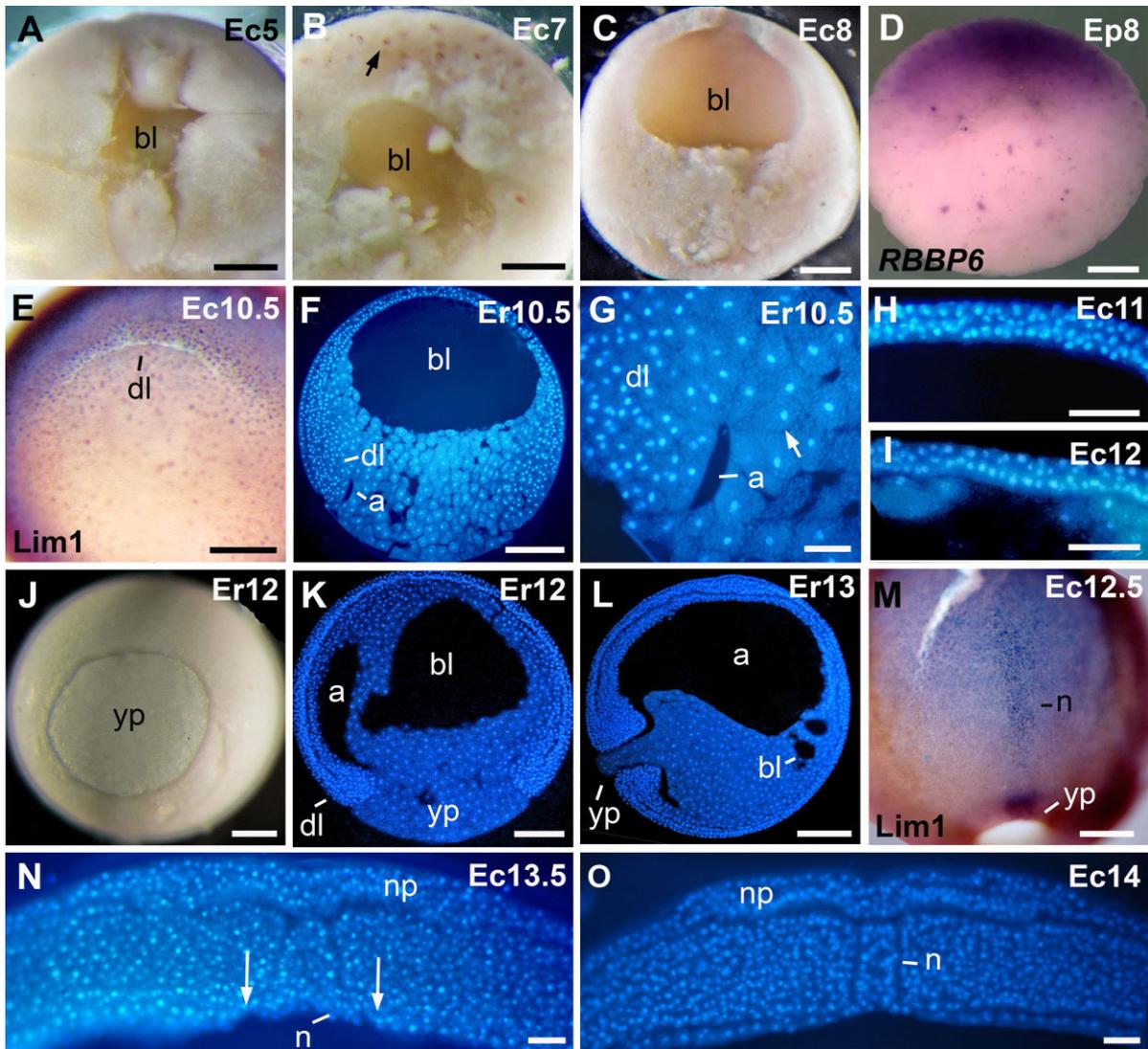

Fig. 2.

Fig. 3. Morphology of early embryos. **A:** Blastocoel of a 16-cell embryo. **B:** Blastocoel of a large-cell blastula. The arrow signals a darkly pigmented nucleus. **C:** Blastocoel of a medium-cell blastula. **D:** *RBBP6* in situ hybridization signal is in the animal hemisphere. **E:** Lim1-positive nuclei occurred in the dorsal blastopore lip. **F:** Sagittal section of an early gastrula. **G:** Higher magnification from the embryo in F. The arrow signals a bottle cell. **H:** Three cell layers in the blastocoel roof of a mid gastrula. **I:** Two cell layers in the blastocoel roof of a late gastrula. **J:** Blastopore of a late gastrula. **K:** Sagittal section of a late gastrula. **L:** Sagittal section of a stage-13 embryo. **M:** Lim1-positive notochord of a late gastrula. **N:** Transverse section through the caudal region of a late gastrula. Arrows indicate the lateral endodermal crests at the limits of the gastrocoel roof plate. **O:** Transversal section through the rostral region of an early neurula. The endoderm covered the archenteron roof. a, archenteron; bl, blastocoel; dl, dorsal lip; n, notochord; np, neural plate; yp, yolk plug. Scale bars = 50 μm in G,N,O; 100 μm in H,I; 200 μm in A–D,E,M; 250 μm in F,J,K,L.

Fig. 1. External views of embryos from cleavage to the neurula. **A:** Eggs within the foam-nest. **B:** Four-cell stage. **C:** Eight-cell stage. **D:** Sixteen-cell stage. **E:** Thirty-two cell stage. **F:** Large-cell blastula. Nuclei were darkly pigmented (arrow). **G:** Medium-cell blastula. **H:** Early gastrula. **I:** Mid gastrula. **J:** Late gastrula. **K:** Late gastrula with a small yolk plug. **L:** Stage-13 embryo that shows formation of the neural groove. This embryo has a yolk plug. Other embryos had a slit blastopore. **M:** Early neural fold stage. **N:** Mid neural fold stage. **O:** Caudal view of the embryo in N. **P:** Closure of the neural tube. The pink color of embryos is an artifact of fixation. In this and the following figures, numbers in the top right-hand corner give the developmental stage, and letters indicate the species: Ec, *E. coloradorum*; Ep, *E. pustulosus;* Er, *E. randi*. b, blastopore; c, cleavage furrow; dl, dorsal lip; f, jelly-foam; ng, neural groove; np, neural plate; nt, formation of the neural tube; yp, yolk plug. Scale bars = 300 μm in B–P; 500 μm in A.

Fig. 2. External views of embryos from tail bud to hatching. **A:** Tail bud stage. **B:** Embryo at the muscular response stage. **C:** Dorsal view of the embryo in B. **D:** Embryo at the circulation to the external gills stage. The trunk acquired some dark pigment. **E:** Head region of a stage-22 embryo. Dark pigment was detected in the head region. **F:** Embryo at hatching. **G:** Higher magnification of the head region from the embryo in F. The external gills reached their maximum length. br, branchial arch; g, gills; tf, tail fin. Scale bars = 300 μm in A; 400 μm in E; 500 μm in G; 600 μm B–D; 1 mm in F.
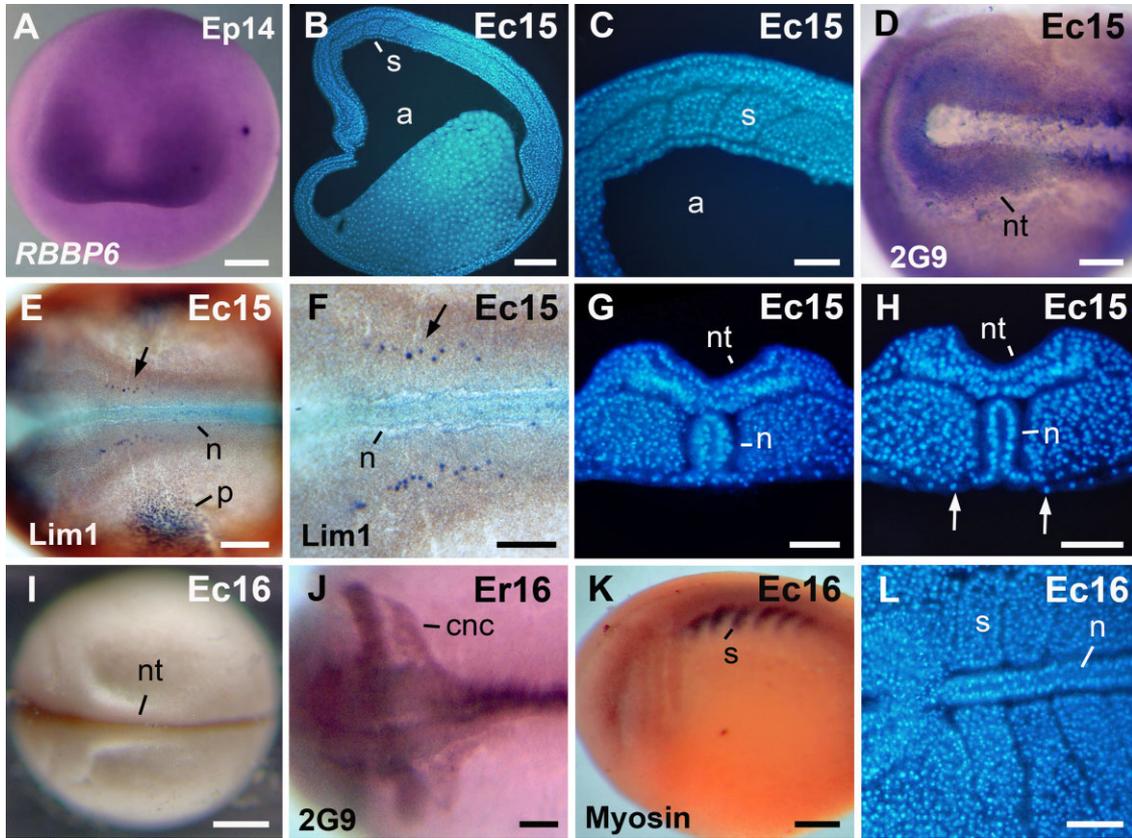
Developmental Dynamics

Fig. 4.

may have favored the acceleration of early development and, consequently, the overlap of developmental process during gastrulation. Although early development of túngara frogs closely resembled the developmental pattern of *X. laevis,* more advanced embryos greatly differed from *X. laevis.* The external morphology of advanced embryos of *Engystomops* resembled the morphology of *Rana* embryos (Pollister and Moore, 1937), with a major difference in pigmentation, as foam-nest embryos of túngara frogs lack dark surface pigment.

Túngara frog embryos were staged according to the *X. laevis* table of stages only until st 14 (Nieuwkoop and Faber, 1994). Thereafter, the embryonic morphology differed from *X. laevis.* Differences detected included the general shape of tail bud embryos (st 17), pattern of somitogenesis, and size of the cranial neural crest cell streams. Somitogenesis involves numerous small cells and cell intercalation in *E. coloradorum* and *E. randi,* whereas in *X. laevis,* each somite consists of cells, which are already elon-
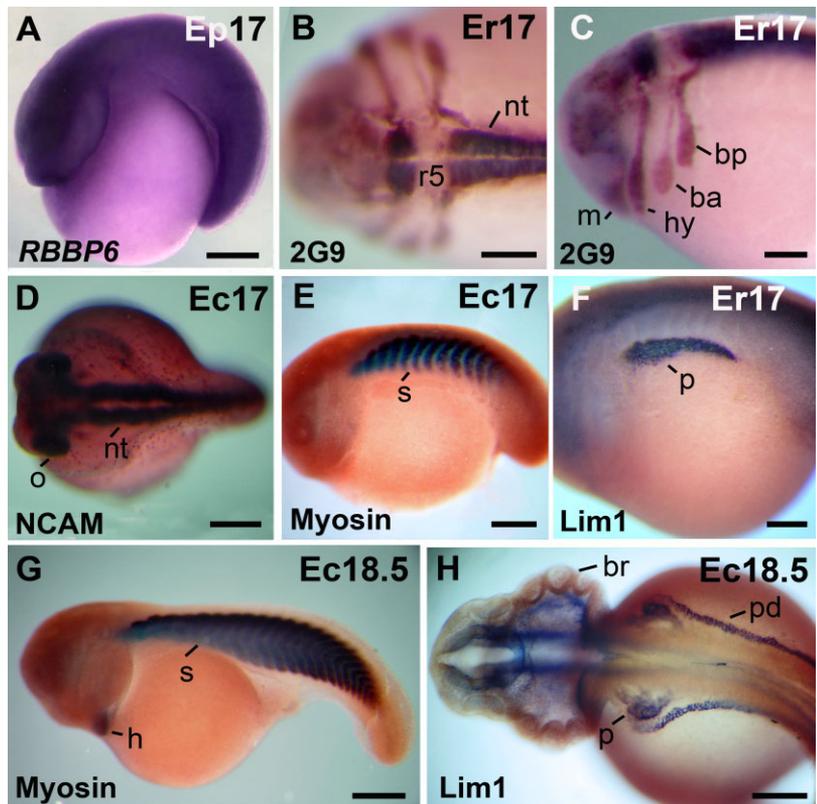

Fig. 5.

gated, and the mode of somitogenesis involves cell rotation (Radice et al., 1989; del Pino et al., 2007). Moreover, the neural plate and neural folds of túngara frog embryos are larger than in *X. laevis*. The cranial neural crest cell streams of *E. randi* embryos are also more conspicuous than in *X. laevis* embryos and are comparable to the pattern observed in the marsupial frog *G. riobambae* (del Pino and Medina, 1998; del Pino et al., 2007). Therefore, although frogs of the genus *Engystomops* and *X. laevis* develop rapidly, and have a similar morphology of early development, there are important differences in their advanced morphogenetic patterns.

Methods for the Study of *Engystomops* Development

Methods used to study *X. laevis* development (Sive et al., 2000) were successfully adapted to analyze the embryogenesis of túngara frogs.

Induction of ovulation.

Ovulation in túngara frogs can be induced by adding water to terraria and by water spraying to simulate rain, as explained in the section on maintenance and reproduction. As in *X. laevis,* it is known that *E. pustulosus* responds with ovulation to the administration of human chorionic gonadotropin (hCG, Davidson and Hough, 1969). Additionally, phonotaxis is induced in adult *E. pustulosus* females with hCG, which will eventually cause the female to ovulate (Lynch et al., 2006). Ovulation was similarly triggered in three females of *E. randi* by the subcutaneal administration of three doses of 100, 200, and 300 IU of hCG, respectively. The hormone was administered at 3-day intervals.

Removal of the egg jelly.

We have found that embryos of *E. pustulosus* can be easily released from foam nests with an adaptation of the *X. laevis* de-jellying method (Sive et al., 2000). Foam nests were removed from terraria and placed onto the surface of de-jellying solution (3% cysteine in 33% MMR, pH 7.2) in a wide beaker. The beaker was gently swirled for several minutes. At intervals, embryos dropped from the nest into the solution, and were immediately removed to a dish containing 33% MMR (MMR solution was prepared according to Sive et al., 2000). In some cases, agitation of the foam with forceps hastened release of embryos. Embryos were then reared as per *X. laevis*.

In contrast, embryos of *E. coloradorum* and *E. randi* were maintained within the foam nest, and were gradually removed for analysis. The jelly layers were somewhat liquid and were successfully removed with forceps. In some instances, embryos were chemically dejellied according to the *X. laevis* method (Sive et al., 2000).

Handling of embryos, immunostaining, and time-lapse recordings.

Embryos of the túngara frogs were handled according to *X. laevis* methods (Sive et al., 2000), including time-lapse recordings. To maintain embryos in the foam-nest, we placed the foam-nests of *E. coloradorum* and *E. randi* in deep plastic dishes of about 15 cm in diameter that were half-filled with chlorine-free water. Dishes were covered with plastic film to prevent desiccation and were maintained at room temperature (18–22°C). Some embryos were moved to a Petri dish filled with 15% Steinberg's solution (Rugh, 1962) to study embryogenesis. Procedures for fixation, vibratome sectioning of embryos, and immunostaining were previously described (del Pino et al., 2004; Venegas et al., 2009).

Injection of mRNA, gene isolation, and in situ hybridization.

Injections of mRNA into early cleavage stage embryos were straightforward using the same method employed for *X. laevis* (not shown) (Sive et al., 2000). We have also adapted the *Xenopus* in situ hybridization method. We cloned a partial cDNA for the *RBBP6* gene out of *E. pustulosus*, and by in situ hybridization we found it to be expressed in the animal region of the blastula (Fig. 3D) and neural tissues, especially the presumptive eye (Figs. 4A, 5A). We have also performed in situ hybridization to the *Shroom2* gene (Lee et al., unpublished data).

Maintenance and Reproduction in Captivity

Tadpoles, juveniles, and adults of *E. pustulosus* and *E. randi* were kept in terraria, with successful reproduction. Maintenance in captivity of *E. pustulosus* at the University of Texas, Austin, differed from the method em-

Fig. 4. Morphology of the neurula. **A:** Neurula stage, anterior view, dorsal to the top. In situ hybridization signal of *RBBP6* was detected in the presumptive eye region. **B:** Para-sagittal section through the somites. **C:** Higher magnification, of the embryo in B. **D:** The antigen 2G9–positive neural folds. **E:** The Lim1-positive notochord, cns cells, and pronephros anlage in a stage-15 embryo. **F:** Higher magnification of the embryo in E. The arrows in E,F signal a cns Lim 1-positive nucleus. **G:** Transversal section through the rostral region. The archenteron roof is covered by endoderm. **H:** Transversal section through the caudal region. The notochord is exposed in the gastrocoel roof plate. Arrows signal the lateral endodermal crests. **I:** A late neurula in dorsal view. **J:** The antigen 2G9–positive neural tube and cranial neural crest cell streams. **K:** Embryo immunostained against sarcomeric meromyosin (indicated as Myosin in the image). **L:** Horizontal section through the somites. a, archenteron; cnc, cranial neural crest; n, notochord; nt, neural tube; p, pronephros anlage; s, somite. Scale bars = 100 μm in C,F–H,J,L; 200 μm in D,E; 250 μm in A,B,K; 400 μm in I.

Fig. 5. Morphology of tailbud embryos. **A:** *RBBP6* in situ hybridization signal was detected in the neural tube. **B:** Dorsal view of an embryo immunostained against antigen 2G9. Rhombomere 5 is 2G9-negative. **C:** Lateral view of the embryo in B that shows the streams of cranial neural crest. **D:** Dorsal view of an embryo immunostained against NCAM. The neural tube and optic vesicles are NCAM-positive. **E:** Somites are sarcomeric meromyosin–positive. **F:** The Lim 1–positive pronephros. **G:** Stage-18 embryo. The somites and heart were positive for sarcomeric meromyosin (sarcomeric meromyosin is indicated as Myosin in the images E,G). **H:** Stage-18.5 embryo. The Lim 1–positive pronephros and pronephric ducts are Lim 1 positive. The Lim 1–positive cns cells are not shown. ba, branchial anterior stream of cranial neural crest cells; bp, branchial posterior stream of cranial neural crest cells; br, branchial arch; h, heart; hy, hyoid stream of cranial neural crest cells; m, mandibular stream of cranial neural crest cells; nt, neural tube; o, optic vesicle; p, pronephros; pd, pronephric duct; r5, rhombomere 5; s, somite. Scale bars = 200 μm in B,C,F,H; 300 μm in A; 400 μm in D,E; 500 μm in G.

ployed with *E. randi* at the Pontificia Universidad Católica del Ecuador. Both methods are described.

The *E. pustulosus* rearing laboratory at The University of Texas, Austin is an adaptation of the enclosures used at the National Aquarium in Baltimore (MD) and the San Antonio Zoo (TX). The laboratory has a daily light cycle of 12 hr and is maintained at 27–28°C with humidity at 30–50% year round. Terraria are placed on wooden frames with a downward angle of 30° and include 5.5-, 10-, and 15-gallon glass aquaria that have a hole with a connector and plastic tubing to allow for drainage. A 2" layer of autoclaved and rehydrated sphagnum moss covers the bottom of each terrarium. Moss is hydrated using room temperature chlorine-free water. Plastic huts made of plant pots and artificial plants are placed in terraria to act as refugia. Terrarium covers are made of plastic frames with mesh screens and lined with Velcro and weather-stripping to prevent escapes.

Reproduction is induced by adding a water pond (small container with rocks and chlorine-free water), increasing humidity, and sometimes simulating rainfall by spraying the terraria with chlorine-free water. Pairs produce a foam nest that is then transferred to a 5-gallon aquarium filled with chlorine-free water.

Tadpoles hatch after 2 days.

Tadpoles are housed in aquaria filled with chlorine-free water and each day are fed JurassiDiet, a pellet food for aquatic reptiles. Within 6 weeks, there are newly metamorphosed frogs. These frogs are fed wingless *Drosophila* only, while juvenile and adult frogs are fed a combination of *Drosophila* and 7-day hatched crickets three times per week.

Engystomops randi was maintained at the Herpetology Section of the Museum of Zoology of Pontificia Universidad Católica del Ecuador. Frogs were kept in terraria, which were stacked in shelves inside a room with controlled environmental conditions. The daily light-cycle was 12 hr, and room-temperature fluctuated between 24–28°C. Terraria measured 60 × 35 × 35 cm and were arranged as follows: Chlorine-free water filled the floor to a height of about 5 cm. The water was covered with a sheet of sturdy plastic mesh that was sup-

ported by legs. Small-sized gravel partially covered the plastic mesh. Terraria were slightly tilted, resulting in the formation of a shallow water pool of about 1 cm in depth in the gravel-free area. Water was changed every 2 months. Coconut shells and a plant, a *Phylodendrum* sp., provided hiding places. Each terrarium was covered with plastic mesh and two glass plates that were placed slightly apart from each other. This cover arrangement allowed aeration, prevented frogs from breaking away, and insured conditions of high humidity. Terraria with a lower water level did not contain water pools, and were used to keep young frogs. Foam-nests, embryos, and tadpoles were maintained under equivalent conditions of light in 50 × 30 × 30 cm aquaria. The aquaria were half-filled with chlorine-free water, and the water temperature fluctuated between 24–26°C. Pumps provided aeration. Water was changed at weekly intervals.

Tadpoles were fed with a mixture of dried and finely ground plant leaves and invertebrates, as follows: the water fern *Azolla* sp., *Taraxacum, Spirulina, Cyclops, Daphnia,* and *Tubifex*. Newly metamorphosed frogs were fed daily for about 10 days with collembola (*Folsomia candida*). Somewhat larger frogs received newly hatched crickets, *Gryllus* sp*.,* as prey. Adults were fed every other day with 15-day-hatched crickets and *Drosophila*.

The presence of a water reservoir at the bottom of each terrarium was advantageous for the maintenance of substrate humidity. Additionally, when the water level of the reservoir was increased, a water pool was formed, and the frogs used it for reproduction. In contrast, reduction of the water level in the reservoir diminished or eliminated the water pool. Young adults of *E. randi* reproduced often, whereas one-year-old and older frogs reproduced less frequently or not at all.

One terrarium contained 12 frogs (6 males and 6 females) collected from nature. In two additional terraria, we maintained 5 males and 5 female laboratory-raised frogs per terrarium. These frogs belonged to the first and second generations. We observed that reproduction occurred when the level of the water in the reservoir was increased until the pool was flooded. In contrast, reduction of the water level

inhibited reproduction. Accordingly, we changed the water and flooded the terraria to induce reproduction.

The 32 *E. randi* adults produced a total of 80 foam-nests in 2 years (February 2006 to March 2008). The monthly production ranged from 0–16, with an average of 3 ± 4 foam-nests per month (the mean and standard deviation are given). Foam-nests were removed and cultured in aquaria until metamorphosis. Development in the foam-nest took 3 days until hatching (observation of 9 foam-nests). Based on the analysis of 121 tadpoles, the aquatic tadpole stages lasted about one month until metamorphosis (34 ± 6 days; mean and standard deviation are given). A maximum of 20 juveniles were maintained per terrarium. Six months after metamorphosis, young frogs of the first and second generations produced foam-nests, an indication of sexual maturity (193 and 201 days, respectively).

Engystomops randi was successfully maintained in small terraria and reached adulthood in 7–8 months after fertilization. In contrast, Davidson and Hough (1969) maintained from 50 to 400 individuals of *E. pustulosus* in beds of sterilized earth placed in the floor of a room of 8 × 12 feet with controlled conditions of light, temperature, and humidity. Tadpoles of *E. pustulosus* required 3–4 weeks to reach metamorphosis, and young frogs reproduced 2–3 months after metamorphosis (Davidson and Hough, 1969).

Túngara frogs are attractive for developmental work due to the ease of their maintenance in captivity and rapid development. In addition, reproduction can be induced by increasing the environmental humidity and by flooding. The synchronous oogenesis, rapid development, and short life cycle of these frogs are attractive for studies that involve the induction of developmental mutations and genetic studies of development.

EXPERIMENTAL PROCEDURES

Immunostaining Methods

Embryos were immunostained in whole mount against Lim1, neural,

and somite-specific proteins. We used the monoclonal antibody MF-20 (Bader et al., 1982) against adult chicken pectoralis myosin to detect muscle development. The monoclonal antibody (4d) against NCAM from chick brain membranes (Watanabe et al., 1986) was used to detect the neural tube. These two antibodies were obtained from the Developmental Studies Hybridoma Bank (Iowa City, IA). The monoclonal antibody 2G9 against a neural antigen from *X. laevis* (Jones and Woodland, 1989) was used to detect the neural tube and the neural crest (del Pino and Medina, 1998). This antibody was donated by E. A. Jones (University of Warwick, Warwick, UK). Some embryos were immunostained with a polyclonal antibody against Lim1, donated by M. Taira (University of Tokyo, Japan). Secondary antibodies were sheep anti-rabbit IgG and sheep anti-mouse IgG. Both antibodies were conjugated to alkaline phosphatase (Roche Molecular Biochemicals, Mannheim, Germany). Immunostaining was done as previously described (del Pino et al., 2004; Venegas et al., 2009). Some sections were cleared, stained with Hoechst 33258 (Sigma-Aldrich, St. Louis, MO), mounted in glycerol, and examined with fluorescent optics.

In Situ Hybridization

E. pustulosus embryos fertilized naturally were de-jellied in $1/3 \times$ modified Marc's Ringer (MMR) with 3% (w/v) cysteine at pH 7.8. They were fixed at the neurula and tailbud stage with $1\times$ MEMFA and were dehydrated with 100% methanol (according to Sive et al., 2000).

To synthesize a probe for *RBBP6* transcripts (RetinoBlastoma Binding Protein 6), partial *RBBP6* cDNA was cloned into a PCRII vector (Invitrogen) by using FirstChoice RLM-RACE Kit (Ambion) and the probe was synthesized with T7 polymerase (Promega). In situ hybridization for *E. pustulosus* was performed with *X. laevis* in situ hybridization protocol (Sive et al., 2000). *RBBP6*-expressing regions were colorized with alkaline phosphatase (AP) and BM purple AP substrate (Roche).

Frog Collection Sites

Foam nests of *E. pustulosus* were obtained from frogs maintained at The University of Texas at Austin. *E. pustulosus* were collected at various times from the Panamá Canal area in Panamá with permission of the Smithsonian Tropical Research Institute and with scientific collecting permits from Autoridad Nacional del Ambiente, Panamá.

Six couples of *E. randi* were collected from 8 to 23 February 2005 in Ecuador, Province of "El Oro," road to the Puyango Forest. The altitude is 288 m above sea level. The geographic coordinates of this site are W 80.083319, S 3.88184. Three couples of *E. coloradorum* were collected on January 30, 2005 from Ecuador, Province of Pichincha, secondary road near Tinalandia north bank of the Toachi river. The altitude of this site is 938 m above sea level, and the geographic coordinates are W 79.05028, S 0.29546. Frogs were collected by S. R. Ron, G. Romero, and E. Tapia. Authorization 016-IC-FAU-DNBAP-MA from the Ministry of the Environment allowed the collection of frogs from Ecuador.

REFERENCES

Bader D, Masaki T, Fischman DA. 1982. Immunochemical analysis of myosin heavy chain during avian myogenesis in vivo and in vitro. J Cell Sci 95:763–770.

Benítez MS, del Pino EM. 2002. The expression of Brachyury during development of the dendrobatid frog *Colostethus machalilla*. Dev Dyn 225:592–596.

Davidson EH, Hough BR. 1969. Synchronous oogenesis in *Engystomops pustulosus,* a neotropic anuran suitable for laboratory studies: localization in the embryo of RNA synthesized at the lampbrush stage. J Exp Zool 172:25–48.

del Pino EM. 1996. The expression of Brachyury (T) during gastrulation in the marsupial frog *Gastrotheca riobambae*. Dev Biol 177:64–72.

del Pino EM, Medina A. 1998. Neural Development in the marsupial frog *Gastrotheca riobambae*. Int J Dev Biol 42:723–731.

del Pino EM, Ávila ME, Pérez OD, Benítez MS, Alarcón I, Noboa V, Moya IM. 2004. Development of the dendrobatid frog *Colostethus machalilla*. Int J Dev Biol 48:663–670.

del Pino EM, Venegas-Ferrín M, Romero-Carvajal A, Montenegro-Larrea P, Sáenz-Ponce N, Moya IM, Alarcón I, Sudou N, Yamamoto S, Taira MA. 2007. Comparative analysis of frog early development. Proc Natl Acad Sci USA 104:11882–11888.

Duellman WE, Trueb L. 1986. Biology of amphibians. New York: McGraw-Hill. 670 p.

Ewald AJ, Peyrot SM, Tyszka JM, Fraser SE, Wallingford JB. 2004. Regional requirements for *Dishevelled* signaling during *Xenopus* gastrulation: separable effects on blastopore closure, mesendoderm internalization and archenteron formation. Development 131:6195–6209.

Gosner KL. 1960. A simplified table for staging anuran embryos and larvae with notes on identification. Herpetologica 16:183–190.

Grant, T, Frost DR, Caldwell JP, Gagliardo R, Haddad CFB, Kok PJR, Means DB, Noonan BP, Schargel WE, Wheeler WC. 2006. Phylogenetic systematics of dart-poison frogs and their relatives (Amphibia: Athesphatanura: Dendrobatidae). Bull Am Mus Nat Hist 299:1–262.

Hough BR, Yancey PH, Davidson EH. 1973. Persistence of maternal RNA in Engystomops embryos. J Exp Zool 185:357–368.

Jones EA, Woodland HR. 1989. Spatial aspects of neural induction in *Xenopus laevis*. Development 107:785–791.

Lynch KS, Crews DC, Ryan MJ, Wilczynski W. 2006. Hormonal state influences aspects of female mate choice in the túngara frog (*Physalaemus pustulosus*). Horm Behav 49:450–457.

Moya IM, Alarcón I, del Pino EM. 2007. Gastrulation of *Gastrotheca riobambae* in comparison with other frogs. Dev Biol 304:467–478.

Nieuwkoop PD, Faber J. 1994. Normal table of *Xenopus laevis* (Daudin). New York: Garland Publishing. 252 p.

Pollister AW, Moore JA. 1937. Tables for the normal development of *Rana sylvatica*. Anat Rec 68:489–496.

Radice GP, Neff AW, Shim YH, Brustis JJ, Malacinski GM. 1989. Developmental histories in amphibian myogenesis. Int J Dev Biol 33:325–343.

Ron SR, Santos JC, Cannatella DC. 2006. Phylogeny of the túngara frog genus *Engystomops* (= *Physalaemus pustulosus* species group; Anura: Leptodactylidae). Mol Phylogenet Evol 39:392–403.

Rugh R. 1962. Experimental Embryology: techniques and procedures, 3rd ed. Minneapolis, MN: Burgess Publishing Company. p. 15.

Ryan MJ. 1985. The Túngara frog: a study in sexual selection and communication. Chicago: The University of Chicago Press. 230 p.

Ryan MJ, Rand AS. 2003. Mate recognition in túngara frogs: a review of some studies of brain, behavior, and evolution. Acta Zool Sinica 49:713–726.

Sive HL, Grainger RM, Harland RM. 2000. Early development of *Xenopus laevis*: laboratory manual. Cold Spring Harbor: Cold Spring Harbor Laboratory Press. 338 p.

Taira M, Jamrich M, Good PJ, Dawid IB. 1992. The LIM domain-containing homeo box gene *Xlim-1* is expressed specifically in the organizer region of *Xenopus* gastrula embryos. Genes Dev. 6:356–366.

Taira M, Otani H, Jamrich M, Dawid IB. 1994a. Expression of the LIM class homeobox gene *Xlim-1* in pronephros and CNS cell lineages of *Xenopus* embryos is affected by retinoic acid and exogastrulation. Development 120:1525–1536.

Taira M, Otani H, Saint-Jeannet JP, Dawid IB. 1994b. Role of the LIM class homeodomain protein Xlim-1 in neural and muscle induction by the Spemann organizer in *Xenopus*. Nature 372:677–679.

Venegas-Ferrín M, Sudou N, Taira M, del Pino EM. 2009. Comparison of Lim1 expression in embryos of frogs with different modes of reproduction. Int J Dev Biol (in press).

Watanabe M, Frelinger AL, Rutishauser U. 1986. Topography of NCAM structural and functional determinants. I. Classification of monoclonal antibody epitopes. J Cell Biol 103:1721–1727.

Developmental Dynamics